Received: 7 October 2020 | Revised: 28 May 2021 | Accepted: 1 June 2021

DOI: 10.1002/hyp.14264

RESEARCH ARTICLE

WILEY

Hydrological modelling for assessing spatio-temporal groundwater recharge variations in the water-stressed Amathole Water Supply System, Eastern Cape, South Africa

Spatially distributed groundwater recharge from hydrological model

Annika Nolte[1,2] | Malte Eley[2] | Matthias Schöniger[2] | David Gwapedza[3] | Jane Tanner[3] | Sukhmani Kaur Mantel[3] | Konstantin Scheihing[4]

[1]Department of Earth Sciences, Universität Hamburg, Institute for Geology, Hamburg, Germany

[2]Department of Hydrology, Water Management and Water Protection, Technische Universität Braunschweig, Leichtweiß Institute for Hydraulic Engineering and Water Resources, Braunschweig, Germany

[3]Institute for Water Research, Rhodes University, Makhanda/Grahamstown, South Africa

[4]Department of Water Resources Management and Rights, Oldenburg-East Frisian Water Board, Brake, Germany

Correspondence
Annika Nolte, Department of Earth Sciences, Universität Hamburg, Institute for Geology, Bundesstraße 55, 20146, Hamburg, Germany.
Email: annika.nolte@uni-hamburg.de

Funding information
Bundesministerium für Bildung und Forschung

Abstract

To increase the resilience of regional water supply systems in South Africa in the face of anticipated climatic changes and a constant increase in water demand, water supply sources require diversification. Many water-stressed metropolitan regions in South Africa depend largely on surface water to cover their water demand. While climatic and river discharge data is widely available in these regions, information on groundwater resources – which could support supply source diversification – is scarce. Groundwater recharge is a key parameter that is used to estimate groundwater amounts that can be sustainably exploited at a sub-watershed level. Therefore, the objective of this study was to develop a reliable hydrological modelling routine that enables the assessment of regional spatio-temporal variations of groundwater recharge to discern the most promising areas for groundwater development. Accordingly, we present a semi-distributed hydrological modelling approach that incorporates water balance routines coupled with baseflow modelling techniques to yield spatio-temporal variations of groundwater recharge on a regional level. The approach is demonstrated for the actively managed catchment areas of the Amathole Water Supply System situated in a semi-arid part of the Eastern Cape of South Africa. In the investigated study area, annual groundwater recharge exhibits a high spatio-temporal heterogeneity and is estimated to vary between ~0.5% and 8% of annual rainfall. Despite some uncertainties induced by limited data availability, calibration and validation of the model were found to be satisfactory and yielded model results similar to (point) data of annual groundwater recharge reported in earlier studies. Our approach is therefore found to derive crucial information for efficiently targeting more detailed groundwater exploration studies and could work as a blueprint for orientating groundwater potential exploration in similar environments.

KEYWORDS
Eastern Cape, groundwater, groundwater recharge, hydrological modelling, semi-distributed model, South Africa, water-stress

1 | INTRODUCTION

Many metropolitan regions in South Africa exhibit a strong water supply vulnerability due to their sole dependence on surface water supply systems (Calow et al., 2010; DWA, 2013; Hedden & Cilliers, 2014; Vörösmarty et al., 2010). Growing water demand and increasing severity of droughts require a diversification of water supply sources as a means to enhance water supply security (Hedden & Cilliers, 2014; Kahinda et al., 2010; Kusangaya et al., 2014; Luker, 2017). Groundwater can be a reliable and economic source of water and its role in adding to a diversification of water supply sources is worth investigating more intensively in water-stressed areas of South Africa (Olivier & Xu, 2019).

In areas that are traditionally supplied with water from dam reservoirs, climatological and river discharge time-series are usually available but regional knowledge on groundwater and groundwater recharge is scarce or highly generalized. This is partly due to the complexity of the majority of South Africa's aquifers which are secondary fractured rock aquifers with highly heterogeneous characteristics (Botha et al., 2002; Sami & Hughes, 1996; Steyl & Dennis, 2010; van Tonder & Kirchner, 1990; Woodford & Rosewarne, 2006). As groundwater recharge is the key parameter for assessing the sustainable yield of aquifers, knowledge about the spatio-temporal variations of groundwater recharge is an asset for identifying target areas for detailed groundwater exploration studies (Simmers, 2013). Thus, we present a semi-distributed hydrological modelling approach that incorporates groundwater routines to assess the spatio-temporal variations of groundwater recharge in river catchments that are actively managed, as an essential step for orientating groundwater resources exploration. The presented approach is demonstrated for the Amatole Water Supply System (AWSS) in the Eastern Cape of South Africa.

Groundwater resource feasibility studies are typically carried out at much smaller scales than those for surface water catchments (South Africa manages surface water resources at the fourth-order catchment scale, termed quaternary catchments). This results in a lack of integration between assessments of the two resources and hinders the development of conjunctive use of groundwater and surface water resources. The approach presented in this paper serves as an example for the integration of reliable groundwater recharge routines into a hydrological model to carry out a differentiated spatio-temporal assessment of groundwater recharge in similarly complex and actively managed systems, using publicly available data such as land and soil cover, topography, climatic time-series and streamflow data. The model spans a simulation period of 10 years from July 2007 to the end of 2017. Yielded recharge amounts are set in the context of existing estimates of groundwater recharge in the broader area of work based on previous studies (DWAF, 2005; DWAF, 2008; Sami & Hughes, 1996; van Tonder & Kirchner, 1990). The current investigation paves way for more detailed groundwater potential studies in the region and could work as a blueprint for future studies in similar water-stressed areas dependent on surface water resources that seek diversification of water supply sources to enhance water supply security.

2 | STUDY AREA

2.1 | Regional water management and hydrological setting

The AWSS supplies approximately 1 million people with drinking water with its major beneficiary being the Buffalo City Metropolitan Municipality (BCMM). Water demand in this area has long been met by sufficient surface water resources due to its location at the foot of the Amathole Mountains (Nel et al., 2013). However, the natural water yield is predicted to fall behind the region's water requirement by the end of the current decade largely due to population and economic growth (DWS, 2016). Regional studies predict that increasing temperatures and a higher frequency or severity of extreme events such as droughts, are likely to further reduce the future reliability of the regional surface water availability (Botai et al., 2020; Dube et al., 2016; Mantel et al., 2015). Water levels in the dam reservoirs have been declining critically in recent years and Buffalo City was facing an acute Day-Zero-scenario in 2020 (Daily Dispatch, 2017; Department of Water and Sanitation, 2019; Global Africa Network, 2018). In addition, there are concerns about the water quality of the respective rivers (Adeniji et al., 2019; Chigor et al., 2013; Palmer & O'Keeffe, 1990). Accordingly, the local water boards as well as the regional and municipal governments are seeking suitable reconciliation options (DWAF, 2008; Scheihing et al., 2020).

The AWSS consists of several barrages located either in the Buffalo River catchment or the Nahoon River catchment. In the Buffalo River catchment, four dams are located (from north to south: Maden Dam, Rooikrantz Dam, Laing Dam and Bridle Drift Dam, Figure 1). In the Nahoon River catchment, only the Nahoon Dam is found (Figure 1). The Kubusi River catchment, where the Gubu Dam and the Wriggleswade Dam are situated, is located north-east of the studied catchments but is worthwhile mentioning because it provides intermittent water transfers to the Buffalo and Nahoon catchments. The three rivers are perennial (DWAF, 2008), but smaller reaches like the Yellowwoods River that discharge into the Buffalo River are ephemeral (Owolabi et al., 2020).

Overflow is the only release from most of the reservoirs. In addition, the effluent of nine Waste Water Treatment Works (WWTW)

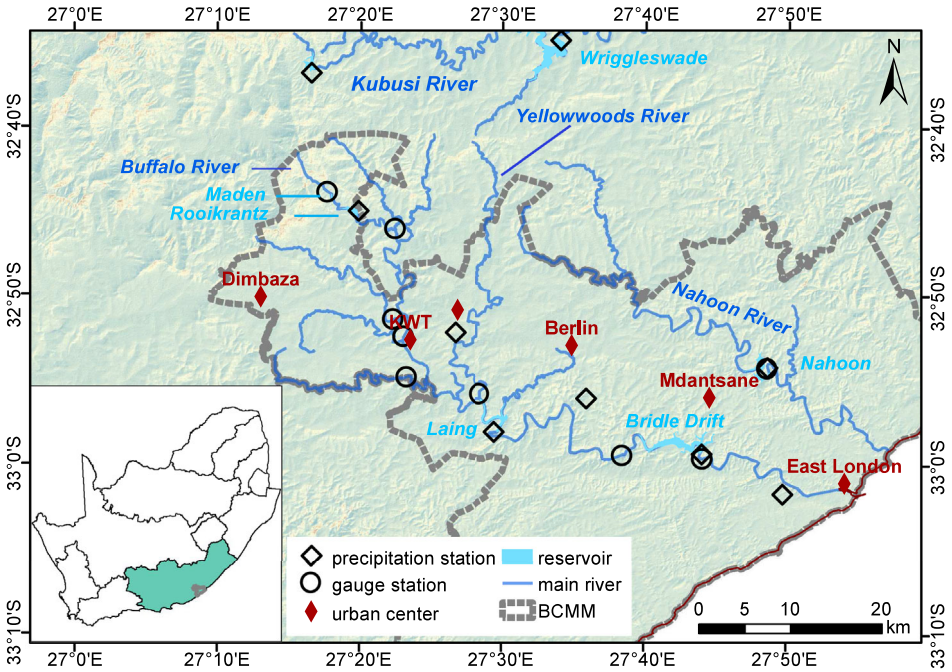

FIGURE 1 Location of the Buffalo City metropolitan municipality (BCMM) in South Africa with its urban centers, main rivers, dam reservoirs as well as gauge and precipitation stations (inset map shows the location of the BCMM in the Mzimvubu to Tsitsikamma water management area (filled green) of South Africa)

contributes to the streamflow in the mentioned rivers (Chigor et al., 2013). The total inflowing volume into these WWTWs was 14.3 Mm^3 a^{-1} in 2005 (DWAF, 2008) and 16.5 Mm^3 a^{-1} in 2016 (BCMM, 2016). Water abstraction for supply purposes takes place at the dam sites. The total annual volume of water available for human consumption from the dammed river water is about 75 Mm^3 a^{-1} (including return flows from WWTWs and excluding water transfers) (DWS, 2016).

2.2 | Physical description

The modelled watersheds (Buffalo River and Nahoon River watersheds – 1279 km^2 and 583 km^2) are situated in the BCMM, located in the central south-eastern part of the Eastern Cape Province, with rivers draining into the Indian Ocean (Figure 1). The topography of the Buffalo River and Nahoon River watersheds is characterized by an increasing elevation from south-east to north-west spanning from sea level to a maximum elevation of approximately 1350 masl in the Amathole Mountains (Figure 2(a)).

In a typical year, rainfall stations in the study area measure between 580 and 815 mm of rainfall (Figure 2(d)), but annual precipitation can be up to 2000 mm a^{-1} in the Amathole Mountain Range (Bailey & Pitman, 2015; Taylor et al., 2016). This implies that the largest portion of annual precipitation falls at the north-eastern border of the investigated catchments. Precipitation variability throughout the annual cycle is high, with the highest rainfall amounts falling in summer between October and March (based on available time-series, referenced in Table A1). The annual average temperature over the simulation period lies in the range of 16–23°C in coastal areas, while inland larger temperature fluctuations are being observed (based on time-series, referenced in Table A1). High evaporation rates throughout the entire year characterize the study area with evaporation rates reaching up to 180 mm per month in summer and reducing to ~50 mm in winter. The mean annual potential evaporation is 1160–1400 mm during the simulation period (Class S Pan evaporation time-series, referenced in Table A1).

The vegetation in the study area consists mainly of closed indigenous forests, and pine and blue gum plantations in the Amathole Mountains. More arid savannah and thicket-like vegetation, grasslands as well as subsistence farming occur from the mountain slopes to the coastal belt (DWAF, 2004, Figure 2(c)).

2.3 | Hydrogeology

Geologically the study area is part of the South African southern Karoo basin. A generalized geological map for the study area is presented in Figure 3. The geology of the study area is dominated by the Middleton and Balfour Formations of the Karoo Supergroup, with widespread dolerite intrusions. The Middleton formation typically consists of mudstones and 30–40% sandstone lithosomes (Johnson, 1976), while the Balfour Formation typically consists of up to 85% mudstones. According to a previous study, no significant primary unconfined aquifers are present in the BCMM (DWAF, 2008). The jointed and fractured aquifers in the southern Karoo basin have been reported to exhibit semi-confined conditions (Dondo et al., 2010; Sami, 1996). Well-developed aquifer sections are largely restricted to fractured zones associated with the dolerite intrusions where high-yielding wells have been reported (Botha et al., 2002; DWAF, 2008). However, most groundwater wells in the area exhibit very low yields with constant flow rates of less than 2 L/s (DWAF, 2008).

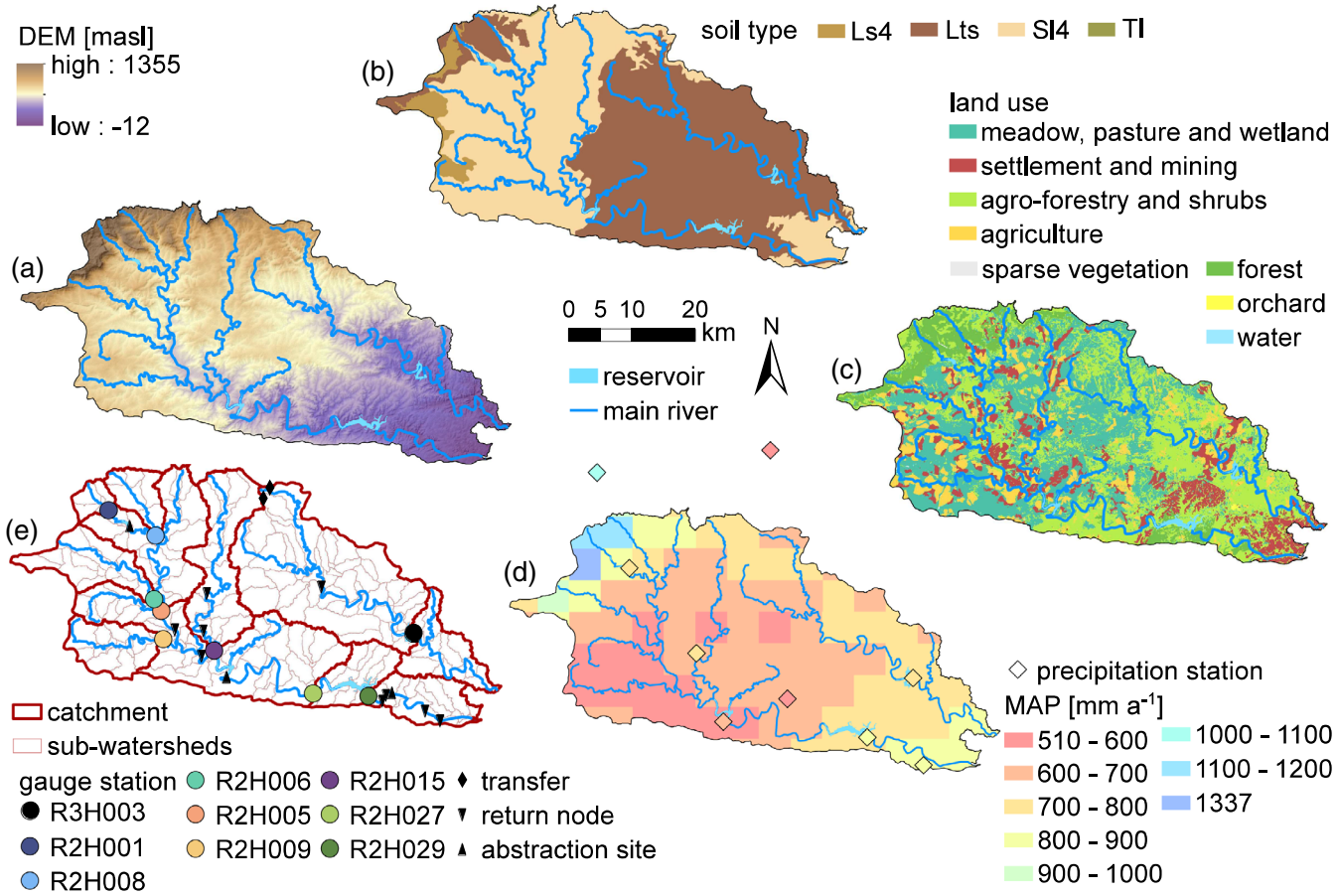

FIGURE 2 (a) Buffalo and Nahoon river catchments that were delineated using a 30 m digital elevation model (DEM), (b) soil type MAP (textural classification: KA4 after Eckelmann et al. (2005)) and (c) land-use MAP (classification: Bossard et al., 2000). (d) Mean annual precipitation (MAP) of the reference grid and MAP of rainfall stations (based on time-series from the simulation period). Sub-watersheds with river gauges and assigned catchment areas generated in the process of calibration (bold printed) and locations of streamflow controlling water management infrastructure. Data sources are referenced and described in Table A1(e) and Table A2(a–d)

Figure 2(b) shows KA4 soil type classification for the study area that corresponds to sandy clay loams (Ls4), clay loams (Lts) and sandy loams (Sl4) (Némétová & Honek, 2017). Those soil types were reported to exhibit fairly-low to low infiltration rates of less than 5–20 mm per hour (Sami, 1992; Sami & Hughes, 1996). The permeability of soils with a sandy (clay) loam texture is generally higher than that of the very fine-textured clay loam soils. It has been observed that soil crusting favours overland flow at hillslopes, with higher portions of water infiltrating in the valley bottom (Nciizah & Wakindiki, 2014; Sami, 1992).

3 | METHODS AND DATA

3.1 | Hydrological model description

The hydrological modelling was carried out using the modelling system PANTA RHEI. It is a deterministic, semi-distributed, physically based hydrological model for long-term or single event simulations. PANTA RHEI has been developed by the Department of Hydrology, Water Management and Water Protection, Leichtweiß-Institute for Hydraulic Engineering and Water Resources, Technische Universität Braunschweig (LWI-HYWAG) in cooperation with the Institut für Wassermanagement IfW GmbH, Braunschweig (LWI-HYWAG & IfW, 2019). The model has been applied in a variety of scientific contexts (Hölscher et al., 2012; Meon et al., 2014; NLWKN, 2019).

PANTA RHEI models the runoff processes on a sub-watershed level. Communication between sub-watersheds takes place via a predefined flow order in which dam structures are conceptually represented as storage units. Mathematical representations of runoff processes transform the input rainfall into the runoff in the model. The respective runoff processes are runoff generation from precipitation, runoff concentration and open channel flow. Using the DYnamic VEgetation SOil Model (DYVESOM) (Kreye, 2015), the discharge response in a river to a rainfall event is modelled by superimposed direct and delayed runoff components (Figure 4). During calibration, individual processes such as the share of the discharge from the lowest soil storage to the interflow and baseflow volumes (P_{eff_U} and P_{eff_B}) are adjusted to the observed discharge by optimizing goodness-of-fit indicators and the fit from simulated to observed runoff curves based on

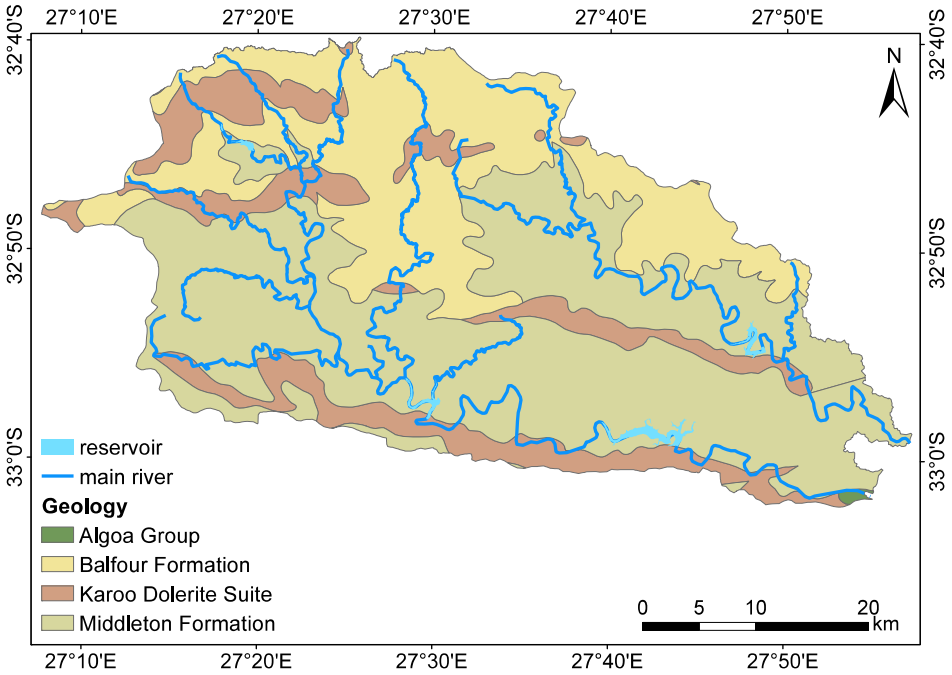

FIGURE 3 Geological map derived from Council for Geoscience (2015) for the Buffalo River and Nahoon River catchments. Balfour and Middleton formation cover a large part of the study area and consist largely of sandstones and mudstones

the preset properties of, for example, soil properties and rooting depth. The net inflow into the groundwater reservoir (groundwater recharge, GWR) can be regarded as equivalent to the baseflow volume on a long-term average under the assumption that groundwater reservoir storage is in a near-steady state in the long-term (Arnold et al., 2000; Lee et al., 2006; Niazi et al., 2017; Zomlot et al., 2015) (Equation (1)). This assumption is justified in the given context as groundwater remains largely unexploited and known private wells are scattered and typically exhibit a very low yield (<2 L/s).

$$\mathrm{GWR} = P_{\mathrm{eff\_B}} = P_{\mathrm{net}} - \mathrm{ET_a} - P_{\mathrm{eff\_D}} - P_{\mathrm{eff\_U}} \quad (1)$$

3.2 | Conceptual model

Dams as storage units are defined by storage-elevation curves and rating curves. Sub-watersheds of an average size of 9 km^2 were generated based on the 30 m DEM in Figure 2(a). They were further discretized into significantly smaller Hydrological Response Units (hydrotopes) based on soil type and land-use.

Streamflow in the modelled Buffalo River and Nahoon River catchments was simulated in the hydrological model as the sum of natural runoff from the catchment area, the inflow from catchment areas upstream, anthropogenic inflows (return flows and transfer), and water abstractions resulting from domestic and industrial demand and irrigation.

The hydrological model was driven by spatially interpolated climatic point data from hydro-meteorological stations. During the simulation, spatial interpolation on a daily timescale was conducted by a combination of Inverse Distance Weighting (IDW) and the Thiessen-polygon-method. Potential evapotranspiration was simulated with a Penman-Monteith approach that accounts for vegetation characteristics at hydrotope level estimated from land-use features and with spatially interpolated time-series of precipitation, humidity, temperature, air pressure, wind velocity and radiation. Figure A1 summarizes the conceptual model set-up.

3.3 | Data used for analysis

The DEM with a resolution of 30 m × 30 m was obtained from the Shuttle Radar Topography Mission (SRTM) dataset. The soil cover and land cover maps are shown in Figure 2(b) and (c), whereby soil parameters were determined from the grain size distribution of the fractions of clay, silt and sand from the Soil and Terrain (SOTER) database of the International Soil Reference and Information Centre (Batjes, 2004). The land-use input class for the model was converted from Landsat eight satellite imagery based on 30 m × 30 m raster cells to European Union Corine Land Cover (Bossard et al., 2000), resulting in eight land-use classes for the study area. Additional information on spatial and other data implemented in the hydrological model can be derived from Table A2.

Information on the locations and names of the stations and data sources from which environmental time-series were retrieved is available in Table A1. Some time-series were disaggregated with linear approaches to a finer temporal resolution to enable simulations on a daily scale and small data gaps were handled with linear interpolation. There were larger data gaps within the meteorological time-series that were filled with long-term daily averages over the simulation period. Continuous time-series provided by the BCMM were combined with incomplete time-series from three other stations. The spatial interpolation of precipitation data required a slightly adapted procedure to deal

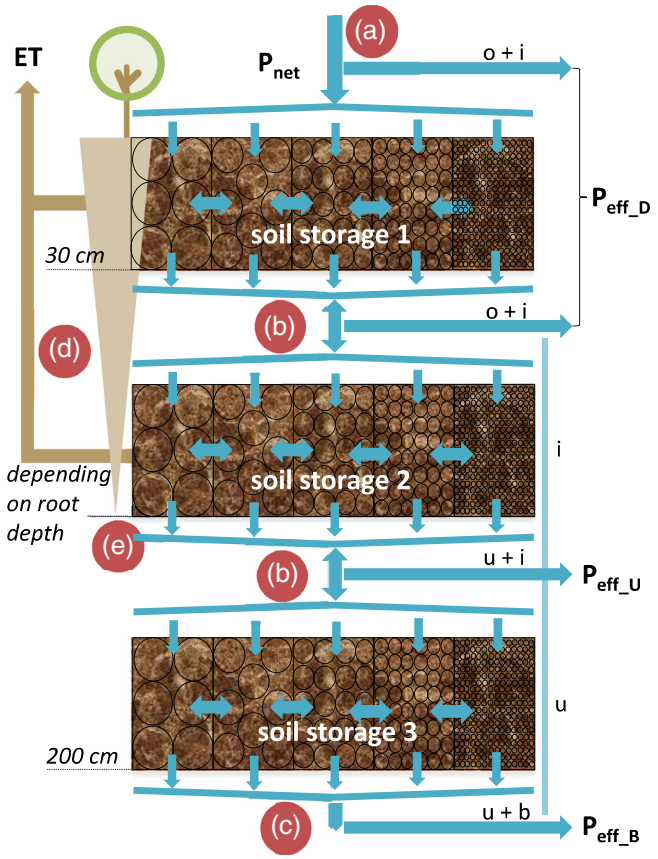

FIGURE 4 DYnamic VEgetation SOil model (DYVESOM) modified from Kreye (2015). The temporal distribution of the water volume from net precipitation (P_{net}, a) can be subdivided into a fraction of direct runoff (formed by P_{eff_D}), a fraction of interflow (formed by P_{eff_U}) and a fraction of baseflow (formed by $P_{eff\text{-}B}$), where P_{eff_D} and P_{eff_U} underlie a certain evapotranspiration ET. The fractions P_{eff_D} and P_{eff_U} are being further subdivided into a delayed component (u) and an instantaneous component (i). Three soil horizons are treated as water storages in the model and are connected by vertical water percolation and capillary rise (b). Groundwater recharge is formed from the lower soil horizon (c). Physical equations with empirical soil parameters drive the mentioned processes of runoff generation. The amount of the actual evapotranspiration ET_a (d) is determined by the potential ET, soil properties and the rooting depth (e)

with the lack of point data for high-elevation areas, where precipitation increases. Rainfall in high-elevation areas was interpolated using a reference map of the MAP (referenced in Table A2) and real precipitation observations at chosen stations (Figure 2(d)). Time-series of estimated precipitation (P_e) were calculated for the centers of the reference map grid cells with an area of 25 km^2 by solving Equation (2). Equation (2) is an estimation method developed in the context of this study, which assumes that the precipitation frequency can be described by data from two nearby stations and the precipitation intensity by the MAP.

$$\sum_{t=1}^{365} P_e = P_{grid} = \sum_{t=1}^{365} (k \cdot w_1 \cdot P_{1,t} + k \cdot w_2 \cdot P_{2,t}) \quad (2)$$

with P_e: estimated rainfall in the center of a reference grid cell; P_{grid}: grid cell value of MAP; $P_{1,t}$ and $P_{2,t}$: rainfall at the two closest stations to the center of a reference grid cell at day t; k: constant factor; w_1 and w_2: weighting factors for station rainfall based on the relative distance to a grid cell

The total number of gauge stations is 16 for the Buffalo River catchment and eight for the Nahoon River catchment. These discharge monitoring sites include nine meters at WWTWs that measure the discharge amounts directed into the treatment plants and two water transfer-meters (for water diverted to the catchments from the Kubusi River catchment). The discharge from WWTW-meters was corrected for 20% water losses due to evaporation during treatment (Haasbroek, 2015). The locations of return flows from WWTWs (return nodes in the hydrological model) were derived from Hughes et al. (2014). Water abstraction rates were derived from time-series of four abstraction-meters from dam reservoirs and a weir downstream of Bridle Drift Dam (Figure 2(e)). Agricultural water abstractions were represented by constant daily water volumes above the gauges for the sub-watersheds that were selected as representative for irrigated land in the lower, middle and upper section of the study area according to officially estimated agricultural water requirements for the year 2005 (DWAF, 2008). Existing evaluations on the operational state of the different gauge stations in the area were used to select suitable gauging sites for model-calibration (Haasbroek et al., 2016 recommend removal or technical revision of some gauges in the study area).

3.4 | Model calibration and validation

The calibration period selected is 2012–2017 (6 years) and the validation period extends from mid-2007 to 2011 (four and a half years). During both periods, both dry phases and extreme rainfall-runoff events, such as a flood in 2011, occurred. The choice of periods can thus be justified on the one hand by a similarly varying rainfall-runoff regime and on the other hand by the fact that data availability was best during these periods. The implementation of a backward validation procedure was due to the need for a hydrologically slightly more diverse calibration period (in terms of rainfall-runoff). The choice of a more hydrologically diverse calibration period ensured that model parameters were adapted to as diverse system states as possible. A set of goodness-of-fit measures (correlation coefficient, model efficiency – based on Nash & Sutcliffe, 1970 – and Root Mean Square Error), expert knowledge of the study area, and visual assessments were used for model calibration and validation.

Parameters of soil hydraulic properties, initial soil water content, storages and rates of runoff concentration, channel retention and interception were adjusted manually within the calibration process at selected gauges displayed in Figure 2(e) (value ranges of adjusted parameters displayed in Table A3). The gauged-catchments in Figure 2(e) define sub-watersheds that were calibrated with the same representative gauge, which means that the calibrated sub-watershed parameters are the same. Results are presented on a

sub-watershed level and not on a smaller hydrotope level because the density of gauges used for calibrating model parameters does not allow a higher spatial resolution. The calibration of the area above R2H008 turned out to be difficult because records of observed streamflow seemed to be too low in comparison with discharge volumes observed at gauge R2H001 (further discussed in the section 4 – chapter 4.1). Other researchers have raised doubts concerning the accuracy of measurements at gauge R2H008 (Haasbroek et al., 2016).

During model calibration, it was assumed that climatic data of radiation and temperature from stations which are situated a few hundred meters lower in elevation than the Amathole Mountain range would lead to an overestimation of calculated potential ET in high elevation areas (no stations can be found in the Amathole Mountains). Hence, the potential ET assumed for high elevation catchment areas was set to be slightly lower compared to available data from meteorological stations further downhill, taking into account the temperature characteristics of the Amathole Mountains (DWAF, 2004). Also, the original rating curve for Rooikrantz Dam was slightly adjusted in our model, using newer storage measurements at the dam gauge.

4 | RESULTS

4.1 | Runoff characteristics and model accuracy

The runoff dynamics in the study area are characterized by significant annual and inter-annual changes that are driven by rainfall variations. The ratio between modelled P_{eff_B} (baseflow) in our study and total runoff lies between 0.01 and 0.12. Consequently, fast runoff concentrations can be observed in the respective hydrographs (Figure 5(a)). The portion of direct runoff in total runoff is relatively high, while the portion of baseflow is quite low. The flow duration curves in Figure 6 confirm this runoff characteristic, yet also show that at most gauges, low flows are sufficiently high to ensure perennial river flow. The mean natural surface runoff coefficient (ratio between rainfall portion that directly forms into runoff and total precipitation) is on average 0.2 but is locally as high as 0.4 (upstream of R2H001).

The manual calibration and statistical evaluation of the model performance was executed by considering correlation coefficients (r), the Nash and Sutcliffe model efficiency index (E) and Root Mean Square Errors (RMSE). The respective values in Table 1 were calculated based on the mean observed and simulated discharge at daily resolution. A medium to strong linear relationship between simulation and observation was confirmed by the correlation coefficient for all sub-catchments. The RMSE shows that the modelled discharge values for the calibration and validation periods differ from the observed discharge by a similar degree. The model efficiency indices lie in a satisfactory range with many values around 0.5 (Nash & Sutcliffe, 1970). Accordingly, the dynamic of rainfall-runoff events were represented well by the discharge simulations throughout each year, as confirmed by the hydrographs and mass curves in Figure 5(a). There are, however, major volume discrepancies in the discharge for individual years. In some cases, these discrepancies are compensated by the alternating under- and overestimations (e.g., R3H003), and in other cases, a single under- or overestimation stands out which results in a long-term volume difference (e.g., sub-catchment R2H001).

Overall, the model quality tends to be better for the Buffalo River catchment, especially in the Upper parts of the catchment. This is confirmed by the respective cross-correlation and duration curves (Figure 6). A sporadically occurring drying of tributaries (e.g., at gauges R2H006 and R2H009) was partly not correctly simulated. These differences lead, for example, to a simulated perennial flow dynamic at the gauge R2H009, which was not always observed.

4.2 | Spatio-temporal groundwater recharge

The hydrological model yields estimates of long-term mean annual groundwater recharge. The calculated groundwater recharge rates range from 2 to 87 mm a^{-1} or 0.3 to 7.9% of MAP (Figure 7(a) and (b)). The highest values for mean annual groundwater recharge are simulated for the catchments in the Amathole Mountains with values of 50–87 mm a^{-1} (or 4–8% of mean annual rainfall). At lower elevations, the maximum values for groundwater recharge are in the range of 10–25 mm a^{-1} (or approximately 2–4% of mean annual rainfall) (Figure 7(a) and (b)). On average, 1.3% of annual precipitation contributes to groundwater recharge (Figure 7(b)). Based on groundwater recharge rates, the total groundwater recharge in the Nahoon River catchment simulated by the model is 0.59 $Mm^3\ a^{-1}$ (5000–15 000 $m^3\ km^{-2}\ a^{-1}$) and in the Buffalo River catchment 1.39 $Mm^3\ a^{-1}$ (2000–87 000 $m^3\ km^{-2}\ a^{-1}$) with high spatio-temporal variations.

Figure 8 provides boxplots of the ranges of inter-annual variations of precipitation, actual evapotranspiration and groundwater recharge for the different sub-watersheds as modelled by the hydrological model. The variability of the annual groundwater recharge generally correlates with the absolute amount of mean annual recharge. Higher absolute recharge amounts are associated with higher relative inter-annual recharge fluctuations (Figure 8). The coefficient of variation (COV) is on average 0.56 for groundwater recharge, which is larger than the COV of precipitation (0.22) and ET (0.20), but smaller than the COV of total runoff (0.68). Extreme precipitation events in 2011 led to statistical outliers for P and ET but not for groundwater recharge.

5 | DISCUSSION

5.1 | Baseflow

The underestimation of baseflow in our model is reflected to some extent in the fact that the BFI calculated in this study is generally lower than in previous studies. The BFI calculated by our model lies, dependent on the sub-catchment, between 0.01 and 0.12. Previously, the BFI was estimated to be between 0.25 and 0.54 in the study area (Hughes et al., 2007; Owolabi et al., 2020) and above 0.18 in other South African catchments with semi-arid climates (Ebrahim &

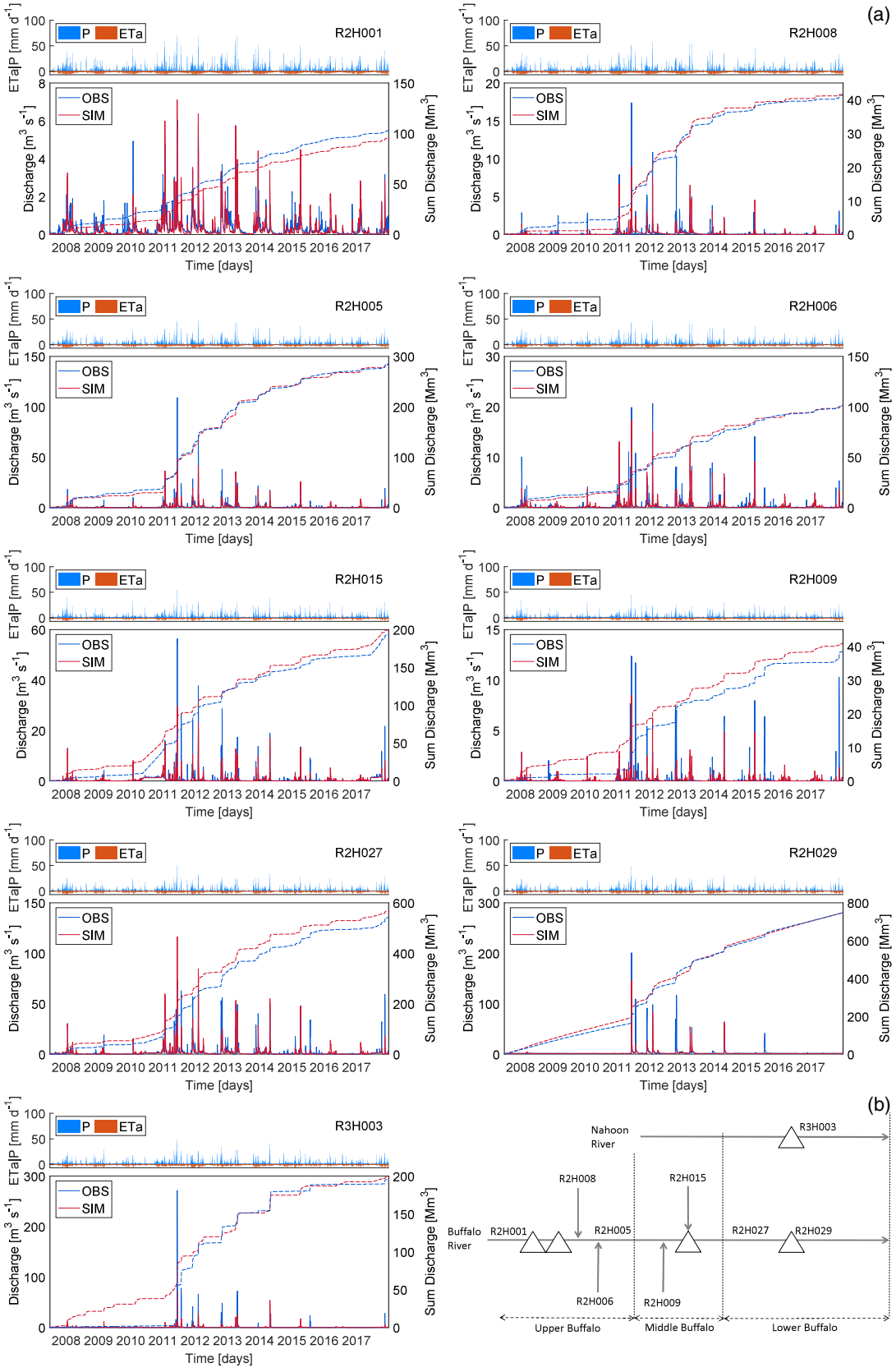

FIGURE 5 (a) Hydrographs and mass-curves of observed and simulated discharge at selected river gauges and simulated areal precipitation (*P*) and actual evapotranspiration (ETa). (b) Sketch of the conceptual model that underlies the discharge simulations with contributing sub-watersheds

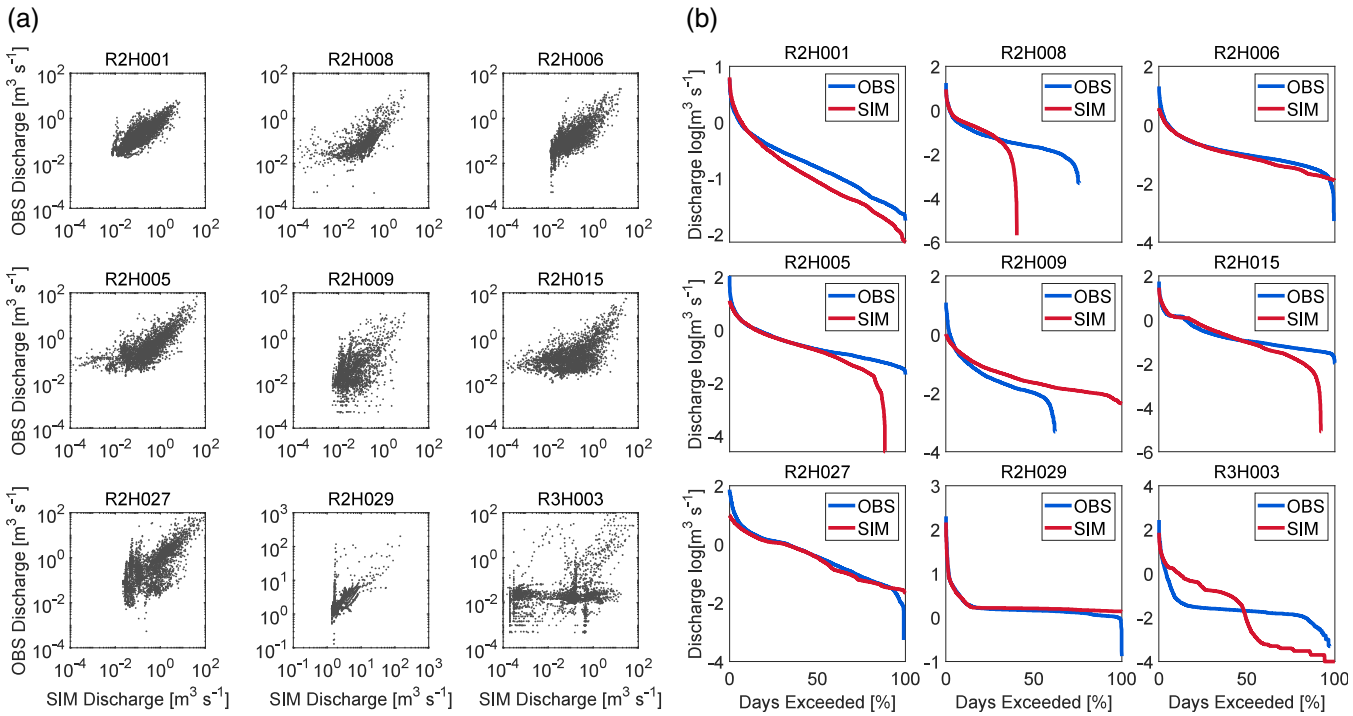

FIGURE 6 (a) Cross-correlation and (b) duration curves of exceedance (exceedance frequencies of discharge values in a certain period of time) of observed and simulated daily mean discharge at river gauges used for calibration (if the discharge is smaller than 1 $m^3 s^{-1}$, the logarithm takes on negative values) in the log-transformed scale

TABLE 1 Goodness-of-fit indices, correlation coefficient (r), model efficiency (E) – Based on Nash & Sutcliffe, 1970 – And root mean square error (RMSE), of calibration (C) and validation (V) time periods of gauges selected for calibration

Gauge	r		RMSE		E	
	C	V	C	V	C	V
Buffalo River						
R2H001	0.81	0.81	0.33	0.36	0.47	0.51
R2H008	0.71	0.79	0.37	0.46	0.49	0.62
R2H006	0.75	0.8	0.69	0.67	0.53	0.62
R2H005	0.76	0.81	2.02	2.82	0.55	0.64
R2H009	0.48	0.66	0.56	0.49	0.21	0.44
R2H015	0.78	0.78	1.26	1.61	0.61	0.61
R2H027	0.72	0.83	3.99	3.66	0.46	0.49
R2H029	0.51	0.77	4.99	5.09	0.18	0.59
Nahoon River						
R3H003	0.53	0.68	3.3	7.63	0.27	0.34

Villholth, 2016). Earlier results indicate that the baseflow could hold a greater share of total discharge in the river system than identified in this study. However, previous results are not directly comparable with the BFI calculated in this study. This is because the baseflow component as modelled in this study refers to a sole groundwater-fed component (see Section 3 – chapter 3.1), whereas the baseflow component in previous studies does not explicitly differentiate between a groundwater-fed part and a part generated by a delayed interflow. This simplification of the baseflow in previous studies may result in a significant overestimation of the pure groundwater-fed baseflow, especially in areas of South Africa with steep topographic gradients (Hughes et al., 2007).

5.2 | Groundwater recharge

The groundwater recharge amounts estimated in this study are presented as long-term mean annual recharge rates. It can well be expected that model errors associated with daily events, as explained above, are compensated for in the long-term when assessing mean annual groundwater recharge. The ranges of annual groundwater recharge rates presented for the different sub-catchments in Figure 8 can in this context be understood as uncertainty bands of the mean annual groundwater recharge estimates that take into account different inter-annual climatic variations and spatial environmental conditions. The importance of intrusive dolerite formations for the constitution of fractured aquifers in the study area was widely recognized in previous studies (DWAF, 2008; Owolabi et al., 2020). Therefore, mean annual groundwater recharge amounts on a sub-catchment level can in reality be heterogeneously distributed within a respective sub-catchment. The estimated GWR in our model represents the averaged GWR over the whole area of each sub-catchment. In total, groundwater recharge volumes are 0.59 $Mm^3 a^{-1}$ in the Buffalo River and 1.39 $Mm^3 a^{-1}$ in the Nahoon River. These volumes are

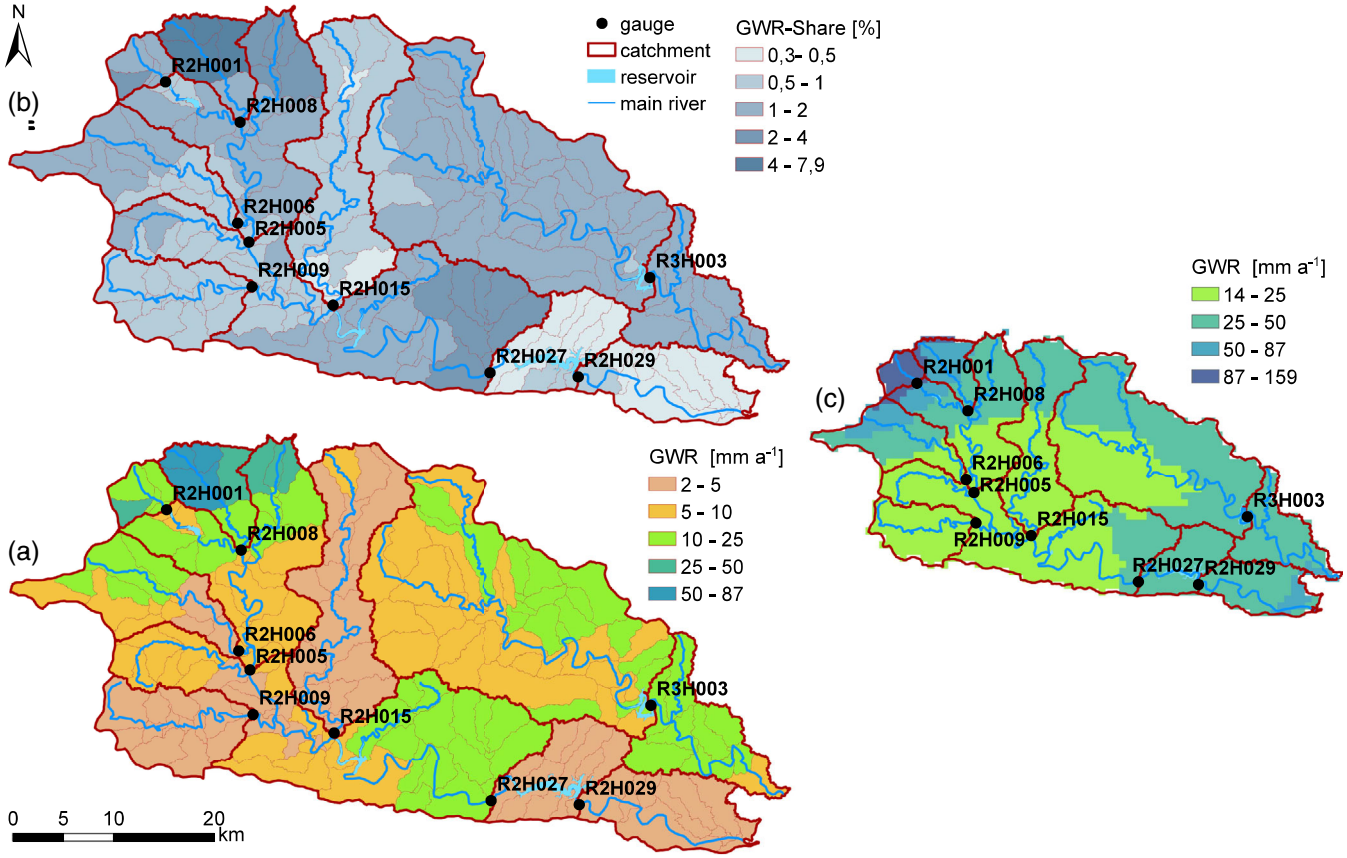

FIGURE 7 (a) Percentage of mean annual rainfall that contributes to mean annual groundwater recharge (sub-watershed level) (b) mean annual groundwater recharge in sub-watersheds. These model results are compared to the recharge grid published by DWAF (2005) (c)

potentially exploitable in a sustainable manner when considering long-term averages, but must be corrected for the existing groundwater withdrawals and the water requirements of groundwater-fed ecosystems.

Compared to the recharge estimates provided in an earlier investigation of the Department of Water Affairs and Forestry (Figure 7(c)), our model results show lower groundwater recharge values for the entire study area. The respective recharge map in Figure 7(c) was developed using the chloride mass balance technique and a GIS-based modelling approach (DWAF, 2005). However, at the same time, the methodology applied in DWAF (2005) has been critically discussed, due to its reliance on spatially limited chloride measurements and multiple interpolation steps (Allwright et al., 2013). A second study that applies the chloride mass balance approach, found that the average recharge in the catchment area of the AWSS is about 2% of precipitation (DWAF, 2008). This value is of a similar magnitude compared to the recharge estimates for many sub-catchments in this study. Also, van Tonder and Kirchner (1990) identified recharge amounts of 2–5% of annual rainfall in semi-arid Karoo formations based on a modified groundwater table fluctuation method. Another study executed in a semi-arid part of the Karoo basin of South Africa - based on a chloride mass balance and an integrated surface-subsurface model – found that recharge in this environment lies between 4.5 and 5.8 mm a^{-1} with high spatial variability (Sami & Hughes, 1996). These results match our findings. With respect to spatio-temporal variations in groundwater recharge, it can be stated that the approach presented here for the AWSS is more reliable compared to previous studies because it is strongly tied to evenly distributed physical parameters (e.g., soil properties, land-use, climate and associated observed discharge). These define interpretable partial runoff processes (such as the groundwater-fed component), which was not the case in previous studies on groundwater recharge in the AWSS.

Overall, the results help to discern on a regional scale sub-watersheds that are expected to exhibit a relatively high groundwater recharge. This information can be used for efficiently targeting more detailed groundwater exploration studies to eventually assess the role that groundwater could play to contribute to water supply source diversification.

5.3 | Model limitations

The modelling approach presented in this paper assumes that recharge is equivalent to groundwater-fed baseflow which is most sensitive to observed streamflow through the calibration process. Accordingly, the model limitations listed below are identified to be the main drivers of model uncertainty concerning the groundwater recharge results that have been presented:

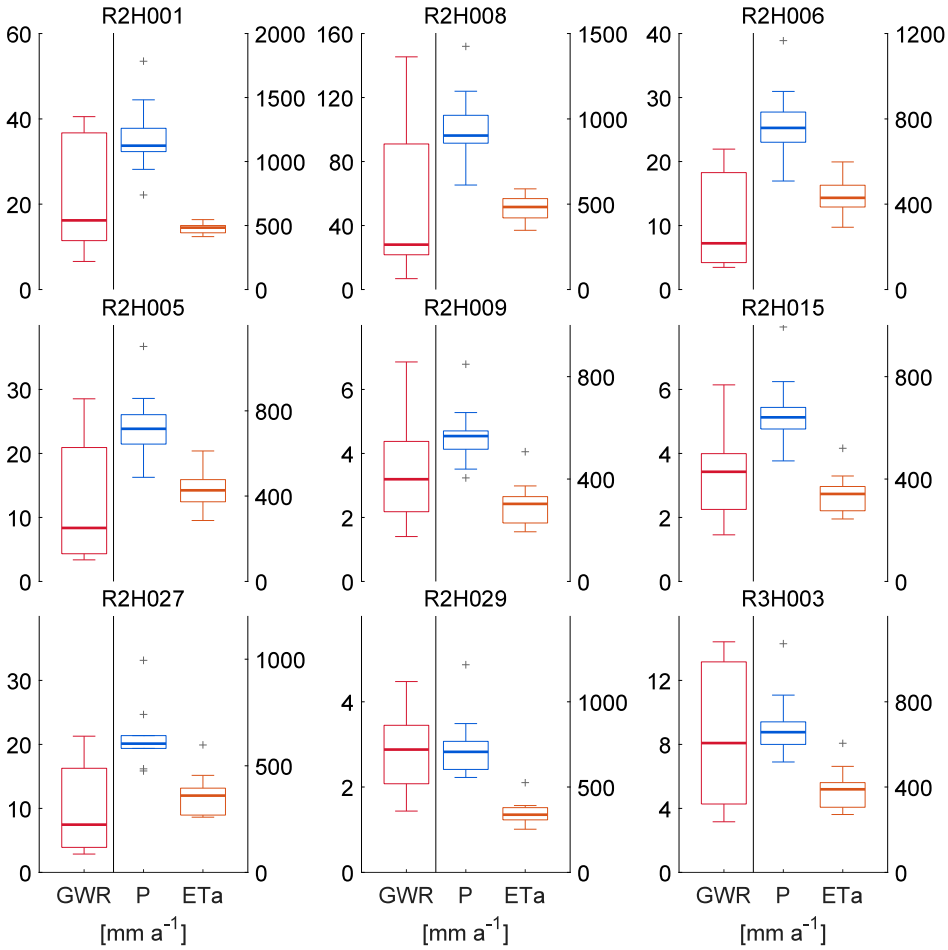

FIGURE 8 Boxplots of model-derived annual groundwater recharge during the period 2007–2017 per sub-catchment, displayed with minimum and maximum (excluding outliers), median, first quartile (25th percentile) and third quartile (75th percentile)

Model limitations result from the following error sources:

1. Unaccounted surface water abstractions by agricultural activity
2. Other human interventions (e.g. arbitrary water releases from dam reservoirs)
3. Errors resulting from the interpolation of precipitation in conjunction with a high topographic heterogeneity
4. Errors associated with soil parameterization based on generalized spatial data

The calibration of the Buffalo River (based on seven well-distributed river gauges) is satisfactory but not good. Due to missing data for actual agricultural surface water abstractions, these abstractions could only be considered in a generalized manner in our model. Potential simulation errors can therefore in part be attributed to unaccounted agricultural surface water abstractions (error source 1) from rivers and streams (no significant groundwater exploitation going on). Unaccounted agricultural water abstraction can be expected to be highest during drought periods when dry conditions increase the irrigation and watering requirements for crops and livestock. Hence, respective unaccounted seasonal water abstractions during dry summer periods will decrease the observed discharge volumes at gauging stations. This error source is not accounted for in our model and could lead to an underestimation of modelled groundwater-fed baseflow amounts in summer periods. However, groundwater-fed baseflow in summer periods is expected to be very low and the inflicted absolute error on modelled mean annual groundwater recharge amounts as done in this study should therefore be minor.

Observed and simulated discharge generally matched better at the gauges where human intervention is low (error source 2). An example of typical model uncertainties encountered as a result of human intervention can be given for gauge R3H003 which is located downstream of the Nahoon Dam. Here, an occasional release of water from below the spill (without specific rules that could be modelled) limits the possibility of correctly simulating the observed discharge amounts. Hence, discharge data from R3H003 only allows evaluation of the river's long-term runoff volume. Accordingly, in the case of the Nahoon catchment, where only a single gauge R3H003 exists, results exhibit the highest uncertainty (Table 1). A better calibration basis for the study area would be achieved with gauged estuaries - which has already been recommended by Haasbroek et al. (2016) and Hughes et al. (2014) – and at least one river gauge in the Nahoon River upstream of the Nahoon Dam.

The necessity to interpolate rainfall amounts over large areas (error source 3), with a low density of observational points, can lead to a blurring of discrete rainfall events, particularly in low elevation areas. Although rainfall sums over larger periods will not be significantly affected by this approach, it can lead to a breakdown of rainfall

amounts from an actual single-day event to a two or three-day event at low elevation. As PANTA RHEI works on a daily resolution, this error source results in the model potentially assuming rainfall on days in certain areas where actually there was no rainfall. Accordingly, in the daily water balance, this error source can lead to an underestimation of baseflow amounts because more frequent rainfall events are represented in the model than actually occurred on a sub-catchment level. This is because the model would then assume occasionally that a portion of the actual daily baseflow as measured includes a component of direct runoff.

Other error sources in our model are likely associated with a low density of meteorological stations and derived rainfall interpolations, and the generation of runoff components in the soil water balance model since this process is highly dependent on soil parameterization. Studies on soil properties and infiltration capabilities from the study area are, however, rare and the soil map used has a low resolution (error source 4).

6 | CONCLUSION

The following conclusions can be drawn from the presented integrated modelling study:

- Runoff characteristics and particularly base-flow dynamics in the investigated catchments can be modelled satisfactorily using the developed hydrological model despite restrictions in data availability.
- The annual groundwater recharge in the coastal South African catchments assessed in this study underlies strong spatio-temporal variations and is largely in accord with previous (point) data on groundwater recharge in the area of work.
- The integration of baseflow modelling techniques in hydrological water balance modelling allows for the spatio-temporal assessment of groundwater recharge on a sub-catchment level, even under several constraints (actively managed barrage system, semi-arid climatic conditions, and dominantly fractured aquifer types). The yielded information on groundwater recharge in turn can support the time- and cost-efficient targeting of more detailed groundwater exploration studies.

ACKNOWLEDGEMENTS

This research was funded by funds of the German Federal Ministry of Education and Research (BMBF) under the funding initiative GRoW (Water as a global resource) and is part of the research project goCAM (Implementing strategic development goals in coastal aquifer management, grand number 02GRW1427C). The authors sincerely thank Nceba Ncunyana, Siyamcela Mamane, Mkhuseli Nongogo and Luthando Mqwabalala of the Buffalo City Metropolitan Municipality as well as Sieg Rousseau from Amatola Water for their support and the provision of municipal data. Further, the authors would like to thank all anonymous reviewers for their constructive contributions.

DATA AVAILABILITY STATEMENT

All model input data sources are referenced in Table 2 and Table 3. Important results generated during this study are available at the HydroShare repository (http://www.hydroshare.org/resource/a8735826b8fe434ca570711a9b9acb49).

ORCID

Annika Nolte https://orcid.org/0000-0001-9562-0728

REFERENCES

Adeniji, A. O., Okoh, O. O., & Okoh, A. I. (2019). Levels of polycyclic aromatic hydrocarbons in the water and sediment of Buffalo River estuary, South Africa and their health risk assessment. *Archives of Environmental Contamination and Toxicology*, *76*(4), 657–669.

Allwright, A., Witthueser, K., Cobbing, J., Mallory, S., & Sawunyama, T. (2013). *Development of a groundwater resource assessment methodology for South Africa: Towards a Holistic Approach* (no. 2048/1). Water Research Commission (Ed.).

Arnold, J. G., Muttiah, R. S., Srinivasan, R., & Allen, P. M. (2000). Regional estimation of base flow and groundwater recharge in the upper Mississippi river basin. *Journal of Hydrology*, *227*(1–4), 21–40.

Bailey, A. K., & Pitman, W. V. (2015). *Water Resources of South Africa 2012 study* (WR2012). Water Research Commission (Ed.).

Batjes, N. H. (2004). SOTER-based soil parameter estimates for Southern Africa. Wageningen. ISRIC - World Soil Information (Ed.).

BCMM. (2016). *Final Draft 2016–2021 Integrated Development Plan Review*. Buffalo City Metropolitan Municipality (BCMM) (Ed.).

Bollrich, G., & Preißler, G. (2000). *Technical hydromechanics 1 [Technische Hydromechanik 1]* (5th ed.). Verlag für Bauwesen.

Bossard, M., Feranec, J., & Otahel, J. (2000). *CORINE land cover technical guide: Addendum 2000*. European Environmental Agency (Ed.).

Botai, C. M., Botai, J. O., Adeola, A. M., de Wit, J. P., Ncongwane, K. P., & Zwane, N. N. (2020). Drought risk analysis in the eastern Cape Province of South Africa: The copula lens. *Water*, *12*(7), 1938.

Botha, J. F., Woodford, A. C., & Chevallier, L. P. (2002). *Hydrogeology of the Main Karoo Basin: Current knowledge and future research needs*. Water Research Commission (Ed.).

Calow, R. C., MacDonald, A. M., Nicol, A. L., & Robins, N. S. (2010). Ground water security and drought in Africa: Linking availability, access, and demand. *Groundwater*, *48*(2), 246–256.

Chigor, V. N., Sibanda, T., & Okoh, A. I. (2013). Variations in the physico-chemical characteristics of the Buffalo River in the eastern Cape Province of South Africa. *Environmental Monitoring and Assessment*, *185*(10), 8733–8747.

Council for Geoscience. (2015). *Geological map of the Republic of South Africa and the kingdoms of Lesotho and Swaziland 2019*. https://www.geoscience.org.za/index.php/2019-03-13-12-40-41/publications/306-geological-maps

Daily Dispatch. (2017). *BCM water restrictions looming* [Press release]. https://www.dispatchlive.co.za/news/2017-04-25-bcm-water-restrictions-looming/

DEA. (2014). *2013–2014 South African National Land-Cover Dataset: DEA/-CARDNO SCPF002: Implementation of land-use maps for South Africa*. Project Specific Data User Report and MetaData (No. 05b). Department of Environmental Affairs (DEA) (Ed.).

Department of Water and Sanitation. (2019). *Water and Sanitation on decline of Eastern Cape dam levels* [Press release]. https://www.gov.za/speeches/water-levelseastern-%20cape-decline-30-jan-2019-0000

Dondo, C., Chevallier, L., Woodford, A. C., Murray, R., & Nhleko, L. O. (2010). *Flow conceptualisation, recharge and storativity determination in Karoo Aquifers, with special emphasis on Mzimvubu – Keiskamma and Mvoti – Umzimkulu Water Management Areas in the Eastern Cape*

and KwaZulu-Natal Provinces of South Africa (No. 1565/1/10). Water Research Commission (Ed.).

Dube, R. A., Maphosa, B., & Fayemiwo, O. M. (2016). *Adaptive climate change technologies and approaches for local governments: Water sector response* (No. TT 663/16). Water Research Commission (Ed.).

DWA. (2013). *National Water Resource Strategy (NWRS): Water for an equitable and sustainable future*. June 2013 Second Edition. Department of Water Affairs (DWA) (Ed.).

DWAF. (2004). *State-of-Rivers Report: Buffalo River System (River Health Programme (2004) No. 8)*. Department of Water Affairs and Forestry (DWAF) (Ed.).

DWAF. (2005). *Groundwater Resource Assessment Phase II (GRAII)*. Department of Water Affairs and Forestry (DWAF) (Ed.).

DWAF (2008). *Development of a Reconciliation Strategy for the Amatole Bulk Water Supply System*. Final Report (No. PWMA 12/R00/00/2608). Department of Water Affairs and Forestry (DWAF) (Ed.).

DWS. (2016). *Amatole Water Supply System Reconciliation Strategy: Status Report: October 2016*. Department of Water and Sanitation (DWS) (Ed.).

Earth Resources Observation And Science (EROS) Center. (2017). *Shuttle Radar Topography Mission (SRTM) 1 Arc-Second Global (Data set)*. https://www.usgs.gov/centers/eros/science/usgs-eros-archive-digital-elevation-shuttle-radar-topography-mission-srtm-1-arc?qt-science_center_objects=0#qt-science_center_objects

Ebrahim, G. Y., & Villholth, K. G. (2016). Estimating shallow groundwater availability in small catchments using streamflow recession and instream flow requirements of rivers in South Africa. *Journal of Hydrology*, *541*, 754–765.

Eckelmann, W., Sponagel, H., Grottenthaler, W., Hartmann, K.-J., Hartwich, R., Janetzko, P., Joisten, H., Kühn, D., Sabel, K.-J., & Traidl, R. (2005). *Manual of soil mapping [Bodenkundliche Kartieranleitung]* (5th ed.). Stuttgart, Germany: Schweizerbart Science Publishers.

Global Africa Network. (2018). *The Eastern Cape is tackling water shortages through new dams and improved controls: A water supply and hydropower project is underway on the Umzimvubu River, but many challenges in the water sector provide opportunities for solution providers in the region* [Press release]. https://www.globalafricanetwork.com/2018/02/15/regions/eastern-cape/tackling-water-shortages-through-new-dams-and-improved-controls/

Haasbroek, B. (2015). *Continuation (2nd period) of the Amatole water supply system reconciliation strategy: 2015 Amatole hydrology and yield update*. Department of Water and Sanitation (DWS).

Haasbroek, B., Mhlanga, L., Pietersen, K., & Jager, G. (2016). Review, evaluation and optimisation of the South African water resources monitoring network (No. WP10871).

Hedden, S., & Cilliers, J. (2014). Parched prospects-the emerging water crisis in South Africa. *Institute for Security Studies Papers*, *2014*(11), 16.

Hölscher, J., Petry, U., Bertram, M., Anhalt, M., Schmidtke, S., Haberlandt, U., & Verworn, A. (2012). Globaler Klimawandel: Wasserwirtschaftliche Folgenabschätzung für das Binnenland. In *Oberirdische Gewässer* (Vol. 33). Norden.

Hughes, D. A., Mantel, S. K., & Slaughter, A. R. (2014). *Informing the Responses of Water Service Delivery Institutions to Climate and Development Changes: A Case Study in the Amatole Region, Eastern Cape (No. 2018/1/14)*. Water Research Commission (Ed.).

Hughes, D. A., Parsons, R., & Conrad, J. E. (2007). *Quantification of the groundwater contribution to baseflow*. Water Research Commission (Ed.).

Johnson, M. R. (1976). *Stratigraphy and sedimentology of the Cape and Karoo sequences in the Eastern Cape Province* (doctoral diss.). Rhodes University, Grahamstown, South Africa.

Kahinda, J. M., Taigbenu, A. E., & Boroto, R. J. (2010). Domestic rainwater harvesting as an adaptation measure to climate change in South Africa. *Physics and Chemistry of the Earth, Parts A/B/C*, *35*(13–14), 742–751.

Kreye, P. (2015). *Mesoscale soil water balance modeling using groundwater measurements and satellite based soil moisture data [Mesoskalige Bodenwasserhaushaltsmodellierung mit Nutzung von Grundwassermessungen und satellitenbasierten Bodenfeuchtedaten]* (doctoral diss.). Technische Universität Carolo-Wilhelmina zu Braunschweig, Braunschweig, Germany. https://publikationsserver.tu-braunschweig.de/receive/dbbs_mods_00061671

Kusangaya, S., Warburton, M. L., van Garderen, E. A., & Jewitt, G. P. W. (2014). Impacts of climate change on water resources in southern Africa: A review. *Physics and Chemistry of the Earth, Parts A/B/C*, *67*, 47–54.

Lee, C.-H., Chen, W.-P., & Lee, R.-H. (2006). Estimation of groundwater recharge using water balance coupled with base-flow-record estimation and stable-base-flow analysis. *Environmental Geology*, *51*(1), 73–82.

Luker, E. (2017). *Transitioning towards water supply diversification: Possibilities for groundwater in Cape Town, South Africa* (Ph.D. thesis). University of British Columbia, Vancouver, Canada.

LWI-HYWAG, & IfW. (2019). *PANTA RHEI User Manual: Program documentation of the hydrological modeling software. [Programmdokumentation zur hydrologischen Modellsoftware]*. (unpublished). Braunschweig. Institut für Wassermanagement IfW GmbH (Ed.).

Mantel, S. K., Hughes, D. A., & Slaughter, A. S. (2015). Water resources management in the context of future climate and development changes: A south African case study. *Journal of Water and Climate Change*, *6*(4), 772–786.

Mantel, S. K., Muller, N. W. J., & Hughes, D. A. (2010). Ecological impacts of small dams on South African rivers Part 2:: Biotic response–abundance and composition of macroinvertebrate communities. *SA Journal of Radiology*, *36*(3), 361–370.

Meon, G., Pätsch, M., & van Phuoc, N. (Eds.) (2014). EWATEC-COAST: Technologies for Environmental and Water Protection of Coastal Regions in Vietnam.

Nash, J. E., & Sutcliffe, J. V. (1970). River flow forecasting through conceptual models part I—A discussion of principles. *Journal of Hydrology*, *10*(3), 282–290.

Nciizah, A. D., & Wakindiki, I. I. C. (2014). Rainfall pattern effects on crusting, infiltration and erodibility in some south African soils with various texture and mineralogy. *Water SA*, *40*(1), 57–64.

Nel, J., Colvin, C., Le Maitre, D., Smith, J., & Haines, I. (2013). *South Africa's strategic water source areas* (no. CSIR/NRE/ECOS/ER/2013/0031/a). WWF-SA (Ed.).

Németová, Z., & Honek, D. (Eds.) (2017). Application of physically-based erosion model in the small catchment of Myjava River basin. Proceedings of the 29th conference of the young hydrologists. Bratislava, Slovakia.

Niazi, A., Bentley, L. R., & Hayashi, M. (2017). Estimation of spatial distribution of groundwater recharge from stream baseflow and groundwater chloride. *Journal of Hydrology*, *546*, 380–392.

NLWKN. (2019). *Globaler Klimawandel - Wasserwirtschaftliche Folgenabschätzung für das Binnenland. Gesamtbericht des Projektes KliBiW Themenbereich Niedrigwasser [Global Climatic Change - Inland water management impact assessment under low flow conditions. General report of the KliBiW project]* (Oberirdische Gewässer Band 42). Hannover. Niedersächsischer Landesbetrieb für Wasserwirtschaft, Küsten- und Naturschutz (NLWKN) (Ed.).

Olivier, D. W., & Xu, Y. (2019). Making effective use of groundwater to avoid another water supply crisis in Cape Town, South Africa. *Hydrogeology Journal*, *27*(3), 823–826.

Owolabi, S. T., Madi, K., Kalumba, A. M., & Alemaw, B. F. (2020). Assessment of recession flow variability and the surficial lithology impact: A case study of Buffalo River catchment, eastern cape, South Africa. *Environmental Earth Sciences*, *79*, 1–19.

Palmer, R. W., & O'Keeffe, J. H. (1990). Downstream effects of impoundments on the water chemistry of the Buffalo River (eastern cape), South Africa. *Hydrobiologia*, *202*(1–2), 71–83.

Sami, K. (1992). Recharge mechanisms and geochemical processes in a semi-arid sedimentary basin, eastern cape, South Africa. *Journal of Hydrology*, *139*(1–4), 27–48.

Sami, K. (1996). Evaluation of the variations in borehole yield from a fractured Karoo aquifer, South Africa. *Groundwater*, *34*(1), 114–120.

Sami, K., & Hughes, D. A. (1996). A comparison of recharge estimates to a fractured sedimentary aquifer in South Africa from a chloride mass balance and an integrated surface-subsurface model. *Journal of Hydrology*, *179*(1–4), 111–136.

Scheihing, K. W., Tanner, J., Weaver, M., & Schöniger, M. (2020). A strategy to enhance management of free basic water via communal taps in South Africa. *Utilities Policy*, *64*, 101043.

Simmers, I. (2013). *Estimation of natural groundwater recharge*. Springer Science & Business Media.

Steyl, G., & Dennis, I. (2010). Review of coastal-area aquifers in Africa. *Hydrogeology Journal*, *18*(1), 217–225.

Taylor, S. J., Ferguson, J. H. W., Engelbrecht, F. A., Clark, V. R., van Rensburg, S., & Barker, N. (2016). The Drakensberg escarpment as the great supplier of water to South Africa. In J. F. Shroder & G. B. Greenwood (Eds.), *Mountain Ice and Water: Investigations of the Hydrologic Cycle in Alpine Environments* (Vol. 21, pp. 1–46). Elsevier.

van Tonder, G. J., & Kirchner, J. (1990). Estimation of natural groundwater recharge in the Karoo aquifers of South Africa. *Journal of Hydrology*, *121*(1–4), 395–419.

Vörösmarty, C. J., McIntyre, P. B., Gessner, M. O., Dudgeon, D., Prusevich, A., Green, P., Glidden, S., Bunn, S. E., Sullivan, C. A., & Liermann, C. R. (2010). Global threats to human water security and river biodiversity. *Nature*, *467*((7315)), 555–561.

Woodford, A., & Rosewarne, P. (2006). *How much groundwater does South Africa have?*. Cape Town, South Africa: SRK Consulting.

Zomlot, Z., Verbeiren, B., Huysmans, M., & Batelaan, O. (2015). Spatial distribution of groundwater recharge and base flow: Assessment of controlling factors. *Journal of Hydrology: Regional Studies*, *4*, 349–368.

How to cite this article: Nolte, A., Eley, M., Schöniger, M., Gwapedza, D., Tanner, J., Mantel, S. K., & Scheihing, K. (2021). Hydrological modelling for assessing spatio-temporal groundwater recharge variations in the water-stressed Amathole Water Supply System, Eastern Cape, South Africa. *Hydrological Processes*, *35*(6), e14264. https://doi.org/10.1002/hyp.14264

APPENDIX A.

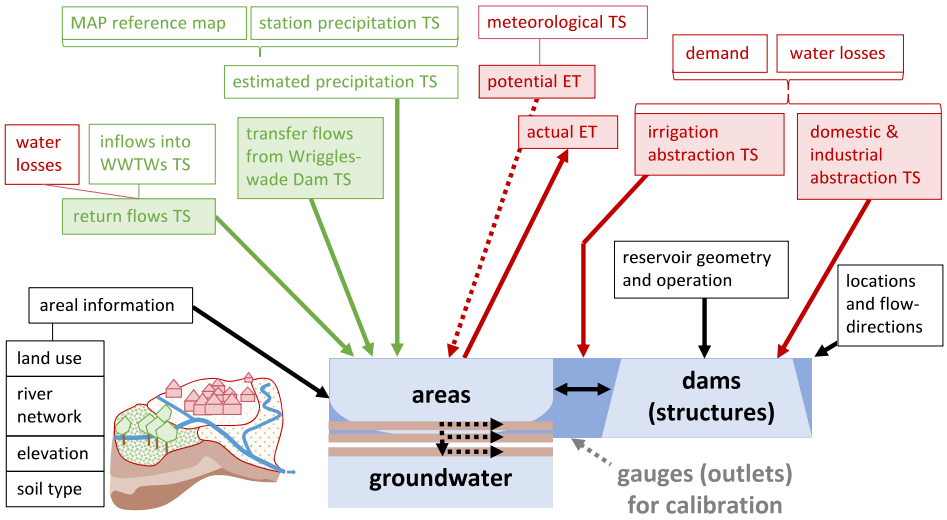

FIGURE A1 Conceptual model: Runoff generation, runoff concentration and open channel flow are processed for sub-watersheds with hydro-meteorological input time-series (TS) taking into account spatial information (locations, flow-directions, sub-watershed and hydrotope properties) and infrastructure information as operation rules, extraction, and injection TS. Calibration and evaluation was performed with observations of streamflow, dam reservoir volume and pan evaporation. Factors adding water to the system are shown in green and factors removing water from the system are shown in red

TABLE A1 Original names, locations, sources and resolution of time-series from the simulation period (SP). Discharge data of river and dam gauges, pipeline gauges ([1] abstraction-meters at barrage locations) and canal gauges (transfer-meters) was downloaded from the Department of Water and Sanitation (DWS) and estimated irrigational water requirements of sub-regions ([3]) from a DWS report. WWTW-meter data and data from an abstraction-meter at bridle drift were derived from the Buffalo City metropolitan municipality (BCMM) as well as evaporation data ([2] locations of return nodes visible in Hughes et al. (2014)). DWS data were available online at http://www.dwa.gov.za/Hydrology/Verified/hymain.aspx

Station	Latitude [dd:Mm:Ss]	Longitude [dd:Mm:Ss]	Source	Time-series	Resolution (years available within SP)
River gauges					
R2H001	32:43:55	27:17:37	DWS	Discharge	Daily (2004–2017)
R2H008	32:46:05	27:22:23		Discharge	Daily (2004–2017)
R2H006	32:51:30	27:22:15		Discharge	Daily (2004–2017)
R2H005	32:52:31	27:22:58		Discharge	Daily (2004–2017)
R2H009	32:54:56	27:23:11		Discharge	Daily (2004–2017)
R2H016	32:56:07	27:26:45		Discharge	Daily (2004–2017)
R2H010	32:56:26	27:27:38		Discharge	Daily (2004–2017)
R2H015	32:55:54	27:28:21		Discharge	Daily (2004–2017)
R2H027	32:59:30	27:38:24		Discharge	Daily (2004–2017)
R2H029	32:59:41	27:44:02		Discharge	Daily (2004–2017)
R3H003	32:54:19	27:48:34		Discharge	Daily (2004–2017)
Dam gauges					
R2R002	32:45:19	27:19:33	DWS	Discharge (spill); Storage volume	Daily (2004–2017)
R2R001	32:58:08	27:29:36		Discharge (spill); Storage volume	Daily (2004–2017)
R2R003	32:59:22	27:43:51		Discharge (spill); Storage volume	Daily (2004–2017)
R3R001	32:54:35	27:48:40		Discharge (spill); Storage volume	Daily (2004–2017)
Pipeline gauges (water abstraction)					
R2H017	1		DWS	Discharge	Daily (2004–2017)
R2H020				Discharge	Daily (2004–2017)
R3H004				Discharge	Daily (2004–2017)
Canal gauges (water transfer)					
R2H025	32:42:53	27:33:11	DWS	Discharge	Daily (2004–2017)
R3H005	32:41:58	27:33:51		Discharge	Daily (2004–2017)
Hydro-meteorological stations					
R2E002	32:58:08	27:29:24	DWS	Precipitation; Evaporation	Daily (2004–2017)
R2E003	32:45:01	27:19:49		Precipitation; Evaporation	Daily (2004–2017)
R2E004	32:59:24	27:43:60		Precipitation; Evaporation	Daily (2004–2017)
R3E001	32:54:17	27:48:35		Precipitation; Evaporation	Daily (2004–2017)
S6E002	32:36:51	27:16:32		Precipitation	Daily (2004–2017)
S6E003	32:34:53	27:34:02		Precipitation	Daily (2004–2017)
Bisho	32:51:45	27:25:64	Agricultural Research Council	Precipitation; Radiation; Temperature; Humidity; Wind speed	Daily (2004/2005–2017)
Berlin	32:56:09	27:35:52	Agricultural Research Council	Precipitation; Radiation; Temperature; Humidity; Wind speed	Daily (2005/2007–2017)
East London	33:01:48	27:49:48	https://en.tutiempo.net/	Precipitation; Temperature; Humidity; Wind speed	Daily (2004–2017)
Bisho			https://www.worldweatheronline.com/lang/de/bisho-weather-averages/eastern-cape/za.aspx	Air pressure	Monthly (2004–2017)
East London			https://www.worldweatheronline.com/lang/de/east-london-weather-averages/eastern-cape/za.aspx	Air pressure	Monthly (2004–2017)

(Continues)

TABLE A1 (Continued)

Station	Latitude [dd:Mm:Ss]	Longitude [dd:Mm:Ss]	Source	Time-series	Resolution (years available within SP)
WWTWs					
Berlin	2		BCMM	Discharge	Daily (2007–2017)
Bisho				Discharge	Daily (2007–2017)
Breidbach				Discharge	Daily (2007–2017)
Central				Discharge	Daily (2007–2017)
Mdantsane				Discharge	Daily (2007–2017)
Potsdam				Discharge	Daily (2007–2017)
Reeston				Discharge	Daily (2007–2017)
Schornville				Discharge	Daily (2007–2017)
Zwelitsha				Discharge	Daily (2007–2017)
Other water abstractions					
Irrigation demand	3		DWAF (2008)	Volume	Annual (2008)
Pumped water from Bridle Drift	1		BCMM	Volume	Monthly (2005–2017)

TABLE A2 Spatial and constant datasets with associated sources, resolution and format. Data were either directly imported into the modelling system, the information was converted or, data was used as a reference

Dataset	Source	Resolution	Format
Topography	Shuttle Radar Topography Mission (SRTM) from Earth Resources Observation And Science (EROS) Center (2017)	30 x 30 m	Raster
Hydrometric data (Rooikrantz, Laing, Bridle Drift and Nahoon dam reservoirs)	BCMM	20 cm spacing (water level)	Table
Hydrometric data (Maden dam reservoir and weir below Bridle Drift)	Hughes et al. (2014); Mantel et al. (2010); Poleni equation after Bollrich and Preißler (2000)	-	Combined information
Land use classes	2013–14 National Land-Cover - 72 classes – documentation: Department of Environmental Affairs (DEA, 2014); available online at http://media.dirisa.org/inventory/archive/spatial/carbon-atlas/phase-ii/2013-14_national_land_cover_72_classes.zip on 01 February 2019	30 x 30 m	Raster
Soil properties (grain size distribution)	Soil and Terrain (SOTER) database of the International Soil Reference and Information Centre (ISRIC) - documentation: Batjes (2004); available online at https://files.isric.org/public/sotwis/SOTWIS_SAF.zip on 01 February 2019	varying	Polygon-shape
MAP	Water Resources of South Africa, 2012 Study (WR2012) - documentation: Bailey and Pitman (2015); available online at https://waterresourceswr2012.co.za/ on 01 February 2019	1.8 x 1.8 km	Raster
GWR	Documentation: DWAF (2005); available online at https://waterresourceswr2012.co.za/ on 12 June 2020	1 x 1 km	Raster
River network and dam reservoirs	Department of Water and Sanitation, South Africa; available online at http://www.dwa.gov.za/iwqs/wms/data/000key2data.asp on 01 February 2019	-	Line-shape/ polygon-shape

TABLE A3 Value ranges of the calibrated parameters of the sub-processes of runoff generation, runoff concentration and open channel flow. More detailed process and parameter descriptions in LWI-HYWAG and IfW (2019)

Runoff generation	Parameter	Range
Base Flow Groundwater Storage	Initial Groundwater Storage Content	500
	Initial Base Flow	0.2–10
Penman-Monteith	Factor ET Potential	0.87–1
Standard Interception	Maximal Interception	2–7
	Maximal Interception Settlements	1
	Emptying Rate	0.1–0.5
Dyvesom1	Slope	1
	Initial Matrix Potential Horizon 1	700–1000
	Initial Matrix Potential Horizon 2	500–700
	Initial Matrix Potential Horizon 3	300–500
	Proportional Surface Runoff	900–2000
	Offset Storage Content	0.2–0.68
	Factor Drying	2
	Factor Percolation	0.5–0.6
	Preferential	0.4–0.75
	Factor ET Actual	1
Runoff Concentration	**Parameter**	**Range**
Unit Hydrograph	Factor ko	2–8
	Factor ki	100–500
	Factor ku	1
	Factor kb	1500–5000
	Water Density	500
	Factor Frost Formation	5
Open Channel Flow	**Parameter**	**Range**
Linear Storage	Factor Retention	1
	Factor Translation	1